Available online at www.sciencedirect.com
SCIENCE DIRECT
International Journal of Heat and Mass Transfer 49 (2006) 2337–2346
International Journal of HEAT and MASS TRANSFER
www.elsevier.com/locate/ijhmt

Bubble slippage on thin wires during subcooled boiling

J.F. Lu, X.F. Peng *

Laboratory of Phase-change and Interfacial Transport Phenomena, Department of Thermal Engineering, Tsinghua University, Beijing 100084, China

Received 3 December 2004; received in revised form 19 August 2005
Available online 2 February 2006

Abstract

An experimental investigation was conducted to observe bubble slippage phenomenon on heating wires during subcooled boiling, and dynamic models were proposed to describe the bubble dynamics and understand the physical nature of these dynamical phenomena. Both experimental and theoretical evidences indicate that the thermocapillary effect of the bubble interface was the most important for the bubble slippage. The drag force caused by bubble motion is considered as the effectual viscosity including viscous effect and thermocapillary force, and it had a linear relation with the bubble velocity. The behavior of the stable bubble slippage and its startup process were theoretically investigated using bubble dynamical models, and different bubble dynamical phenomena were also described and discussed. The theoretical results were in a reasonable agreement with the experimental observations.
© 2005 Elsevier Ltd. All rights reserved.

Keywords: Nucleate boiling; Bubble slippage; Thermocapillary

1. Introduction

Phase change phenomena and associated heat transfer, characterized by small temperature difference and high heat flux, are encountered in various energy conversion and utilization systems. Boiling and condensation have been widely employed to improve the heat transfer performance of heating and cooling devices and/or meet the increasing demand of high heat removal in spacecraft thermal control, aerospace science and technology, electronic cooling, and bioengineering, and so on. These high-technological applications have further promoted more comprehensive investigations on boiling, condensation and other phase change phenomena, particularly, understanding their physical nature.

The earliest work on boiling can be traced back to the Leidenfrost's observation [1], and Nukiyama's work in 1934 [2] described the basic characteristics of pool boiling on a wire, particularly the boiling regimes and associated heat transfer modes. Many researchers focused their investigations on understanding macroscopic phenomena and determining heat transfer performance, such as nucleation, boiling modes and transition, and associated heat transfer enhancement [3,4]. To consider the effect of bubble dynamics in boiling systems, bubble dynamical processes, such as bubble growth and departure were investigated in detail [5–7].

In more recent investigations, the attention has shifted to explore new phenomena associated with microscale effects and/or nanoscale effects [8–10]. Some new high-technological applications of boiling phenomena, like thermal ink jet printer and micro-electro-mechanical systems (MEMS) have made researchers pay more attention to understand bubble dynamical behavior [11]. In these applications, bubble expansion, oscillation and other motion were considered very important factors controlling print quality and associated performance. Meanwhile, bubble slipping was also investigated as one of significant phenomena and dynamical processes in various cases and boiling systems [12]. Wang et al. [13] conducted a series of subcooled boiling experiments on thin Pt wires, and they observed plentiful phenomena, such as bubble sweeping,

* Corresponding author. Tel./fax: +86 10 6278 9751.
E-mail address: pxf-dte@mail.tsinghua.edu.cn (X.F. Peng).

0017-9310/$ - see front matter © 2005 Elsevier Ltd. All rights reserved.
doi:10.1016/j.ijheatmasstransfer.2005.08.036

Nomenclature

A	cross-section area (m^2)
a	acceleration ($m\ s^{-2}$)
B	temperature coefficient of surface tension ($J\ m^{-2}\ K^{-1}$)
C	perimeter (m)
c	thermal capacity ($J\ K^{-1}\ kg^{-1}$)
D	temperature gradient ($K\ m^{-1}$)
f	force (N)
h	convective heat transfer coefficient ($W\ m^{-2}\ K^{-1}$)
l	distance (m)
m	mass (kg)
q	heat generation (W)
q'	linear heat generation ($W\ m^{-1}$)
q''	heat flux ($W\ m^{-2}$)
R	radius (m)
t	time (s)
T	temperature (K)
u	velocity ($m\ s^{-1}$)
V	volume (m^3)
x	coordinate (m)

Greek symbols

α	dimensionless coefficient (–)
θ	angle (rad)
T	temperature difference (K)
σ	interface tension ($J\ m^{-2}$)
κ	thermal diffuse coefficient (m^2/s)
τ	time (s)
λ	conductivity ($W\ m^{-1}\ K^{-1}$)
ρ	density ($kg\ m^{-3}$)
μ	effectual viscosity ($kg\ m^{-1}\ s^{-1}$)

Subscripts

0	initial or reference state
b	bubble
d	driving force
g	gas
i	interface, inertia force
l	liquid
sat	saturated state
w	wire

a variety of jet flows. Their investigations were mostly focused on the observation of experimental phenomena, and only drawn a general description that the sweeping was partially affected by the bubble interaction and mainly induced from the Marangoni effect.

This paper mainly presents experimental observations of bubble dynamical behavior for subcooled liquid boiling on very thin heating wires. An attempt was made to develop theoretical models to describe and understand the bubble slippage phenomenon, and an emphasis was addressed on the behavior of the stable bubble slippage and its startup process. A discussion was also conducted for the comparison of the theoretical predictions with the experimental observations.

2. Experimental observation

2.1. Experiment facility

The experimental facility employed in this investigation mainly included three parts, the test section, power supply and acquisition system, as shown in Fig. 1. The testing vessel with glass window having size of $250 \times 250 \times 400$ mm was made of stainless steel. A platinum wire heater was horizontally installed in the vessel, and the ends of the wire were connected to two electrodes having diameter of 5 mm, respectively. The wires used in this investigation were 80–100 mm long and diameter of 100 μm. A preheater and cooler were employed for adjusting and keeping the bulk liquid temperature approximately invariable and at a specified temperature. The pressure in the vessel was kept at atmospheric pressure. The working liquid was pure water.

The power was supplied using a HP Agilent Model-6031A system, which can provide a maximum voltage of 20 V and maximum power of 1000 W. Direct current was applied to the wire and a uniform heat flux was generated to heat the liquid. To reduce the boundary effect of the electrodes, the voltage of the investigated section was measured directly by the voltage meter, as shown in Fig. 1.

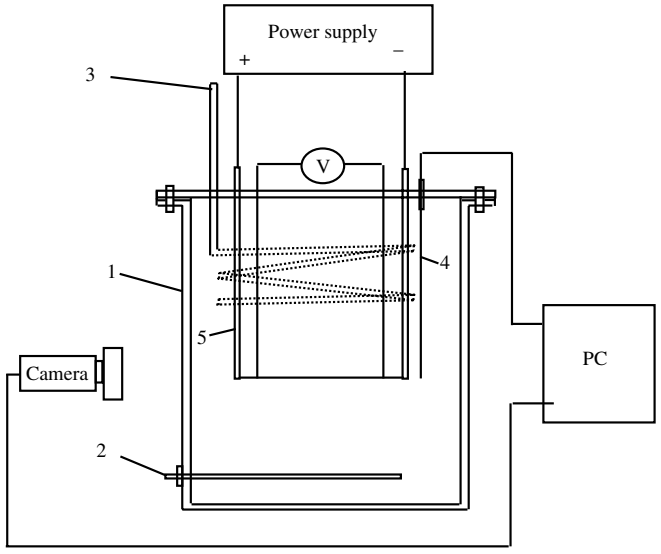

Fig. 1. Schematics of testing system: (1) testing vessel, (2) preheater, (3) cooler, (4) thermocouple, and (5) electrode.

The acquisition system included photo image acquisition and data acquisition system. The photographic system consisted of a high-speed CCD camera (the Motionscope PCI, Redlake imaging), a high-resolution image acquisition card, and zoom lenses. The CCD camera can reach a high speed up to 2000 fps. The present experiments used recording rates of 500 fps, the resolution 320×280 pixels. The images were sent to a computer and stored for further analysis.

The data were collected using the data acquisition system, Keithley 2700 multimeter system, and the error of voltage measurement was less than 0.1 μV (0.005 K for temperature measurement). A T-type thermocouple with a diameter of 0.3 mm was used to measure the bulk liquid temperature, as shown in Fig. 1, and the uncertainty was 0.2 K. The current and voltage applied to the wire were measured to determine the heat flux, and the uncertainty of average heat flux is below 2%. The average wire temperature was then estimated from the wire resistance by the calibrated correlation. The resistance of the wire was approximately a linear function of temperature. So the temperature change of the wire could be obtained from the measurement of the wire resistance. The error analysis shows that the overall uncertainty of the wire temperature measurement was 2 K. It is worth to note that local temperature is of critical importance for recognizing bubble dynamic characteristics.

2.2. General observation

For subcooled liquid boiling on thin wires, the bubble dynamical phenomena mainly include three types: stable large bubble, moving bubble and small bubble jet. Stable large bubbles usually occurred at low heat generation with high subcooling, and they kept stable until they departed from the wires. Fig. 2a presents some stable large bubbles for the bulk liquid temperature of 30 °C at heat flux 0.62×10^6 W m^{-2}. Small bubble jets usually occurred at high heat generation rates, and the bubbles could not keep stable on the wire and departed from the wire quickly. Fig. 2b presents small bubble jet phenomena for the bulk liquid temperature of 30 °C at heat flux 2.53×10^6 W m^{-2}. For these two boiling phenomena, the bubble departure plays an important role in boiling heat transfer, while the effect of bubble motion on the wire can be ignored.

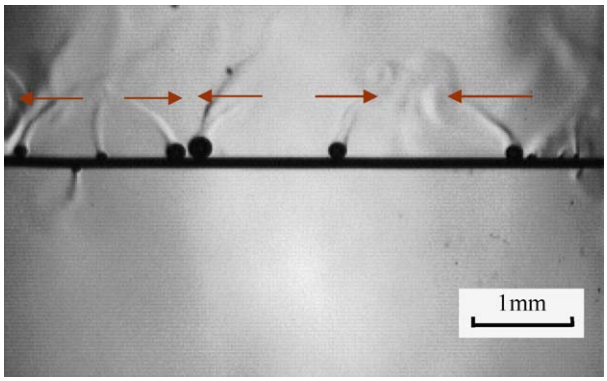

Fig. 3. Bubble slipping and bubble jet flows.

At moderate heat generation rates, many bubbles moved forward or backward when they still kept staying on the wire. Fig. 3 presents bubble slipping and bubble jet flow phenomena on the thin wire, the bulk liquid temperature 30 °C and heat flux 1.5×10^6 W m^{-2}. Different from the stable large bubbles and small bubble jet flows, the bubble motion plays a more important role in the heat transfer during boiling. Since the bubble departure was investigated in many available articles [6,7], the present article will mainly investigate complex bubble dynamic processes on the wire.

A whole bubble dynamical process on a heating wire mainly includes four sub-processes, bubble slippage, separation, collision and oscillation. Bubble slippage is normally a basic process for other dynamical processes. In the experiments, a bubble was observed separating from an immobile bubble or its initial place, and then it usually continued sliding before collision. Bubble collision was also observed frequently, and bubbles might coalesce through bubble collision. The experimental observations also indicate that bubbles could oscillate between bubbles or some

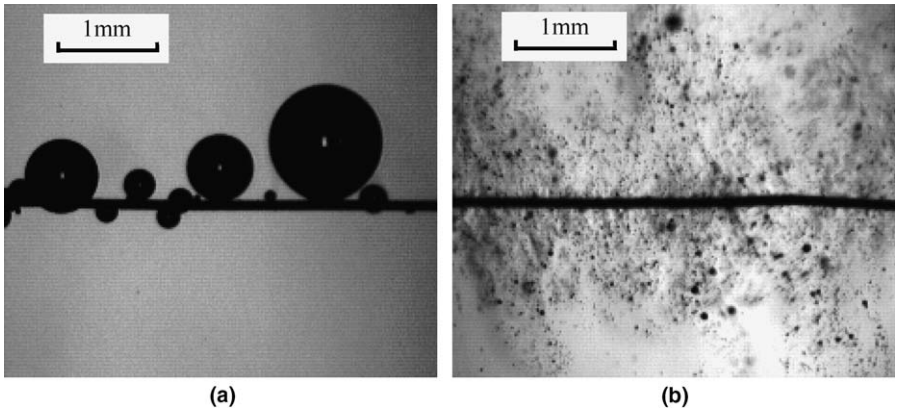

Fig. 2. Bubble dynamic phenomena: (a) stable large bubble and (b) small bubble jet flows.

ends or obstructors on a wire. In some special cases, a bubble was seen skipping during slippage process or at a certain place.

For a moving bubble, its movement influenced much larger area than normal static bubble interaction range, and the boiling within this area should be quite different from other area without bubble motion. Apparently, bubble motion is highly expected to alter the nucleation and bubble dynamical behavior and enhance boiling heat transfer in the influenced areas, and this will be of significance in microscale systems. In present investigation the focus is addressed on the bubble slippage.

2.3. Bubble slippage

Bubble slippage is one important phenomenon and plays an important role in subcooled boiling on a heating wire. The bubble slippage occurs more commonly at liquid temperatures near 40 °C and heat fluxes $0.4–0.8 \times 10^6$ W m^{-2}, and the bubble could slide more than 50 mm.

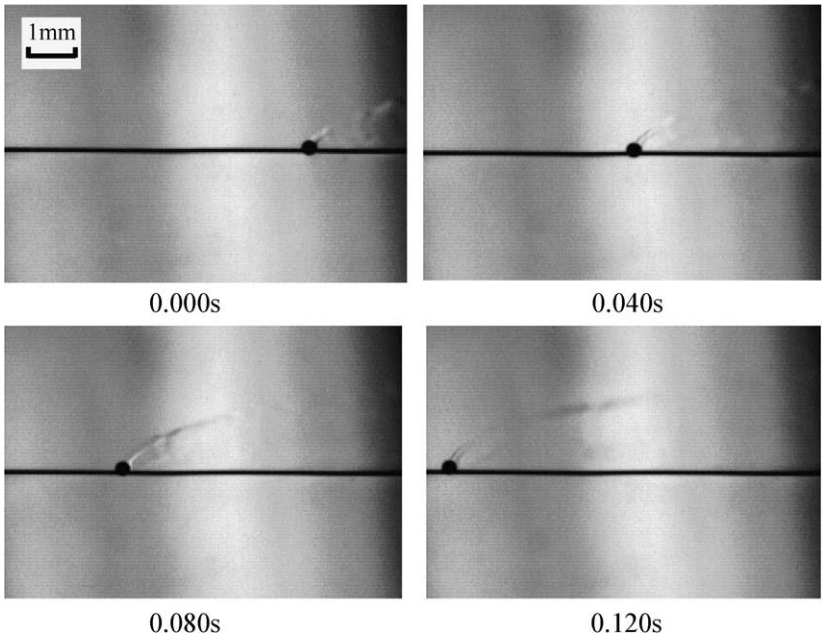

Fig. 4. Small bubble slippage.

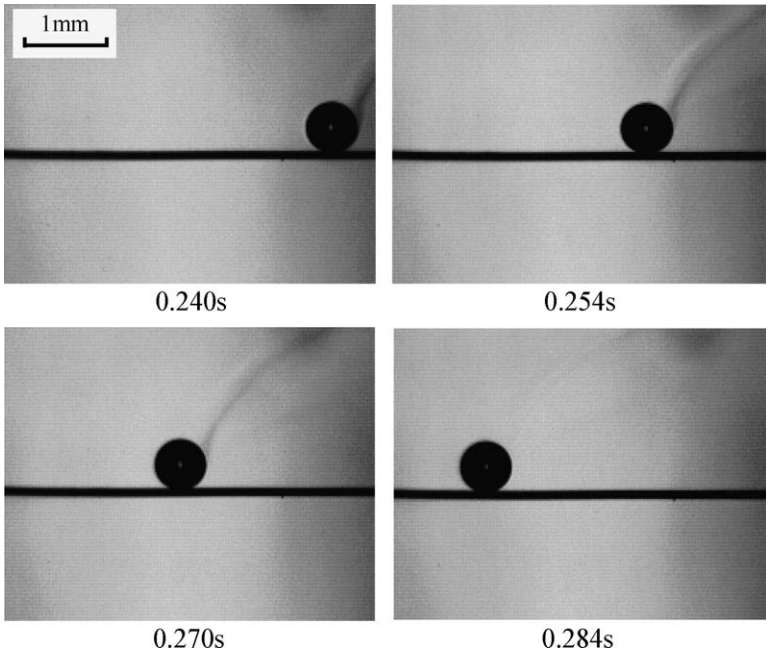

Fig. 5. Big bubble slippage.

The radius of slipping bubbles ranged from 0.05 mm to 0.6 mm.

Fig. 4 presents a bubble slippage having a radius of 0.2 mm from the right side to the left, the bulk liquid temperature 40 °C and heat flux 0.45×10^6 W m^{-2}. The bubble passed 5.4 mm with an almost constant velocity of 45 mm s^{-1}, as the result of line 1 in Fig. 6.

Fig. 5 presents the slippage process of another bubble having a radius of 0.31 mm, the bulk liquid temperature 40 °C and heat flux 0.56×10^6 W m^{-2}. The bubble passed 3.8 mm with an almost constant velocity of 64 mm s^{-1}, as the illustrated line 2 in Fig. 6.

Clearly, the bubbles could slide along the wire for a long distance, and the slipping velocity kept at an almost constant velocity. Apparently, there should exist some strong forces to induce/drive the bubbles against the liquid viscosity.

Under normal conditions, a bubble slippage began with a bubble acceleration process from the bubble initial place. A bubble slippage startup process is illustrated in Fig. 7 for the water with liquid temperature 30 °C and applied heat flux 0.66×10^6 W m^{-2}. Initially the bubble stood on the wire and a jet was just above the bubble. In the next 0.030 s, the bubble separated from the initial place about 0.68 mm, and the jet above the bubble was declined to the opposite direction of bubble moving. From Fig. 7, the bubble grew up and absorbed heat from the wire during accelerating. The change of bubble acceleration and velocity is illustrated in Fig. 8. The bubble accelerated to

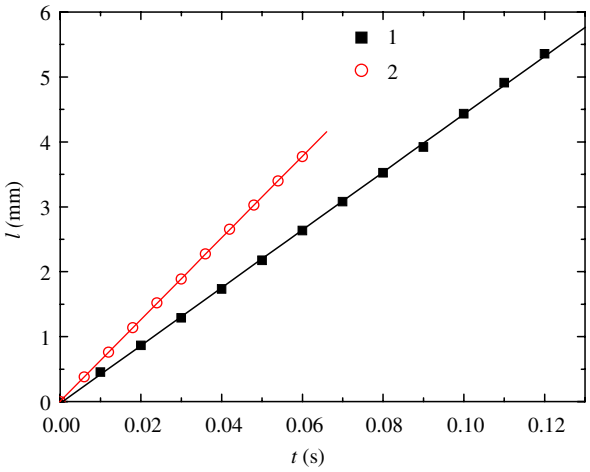

Fig. 6. Bubble slippage distance.

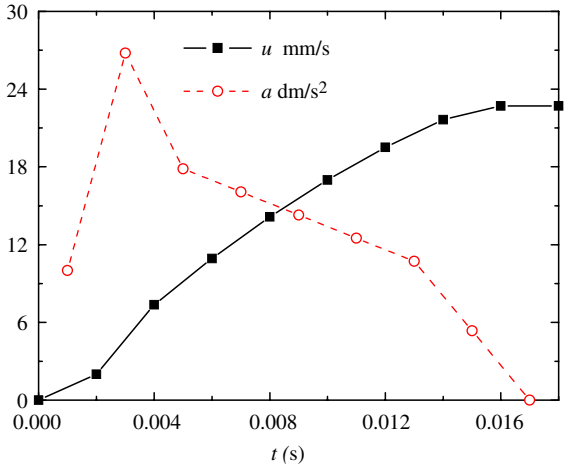

Fig. 8. Change of acceleration and velocity during bubble slippage startup.

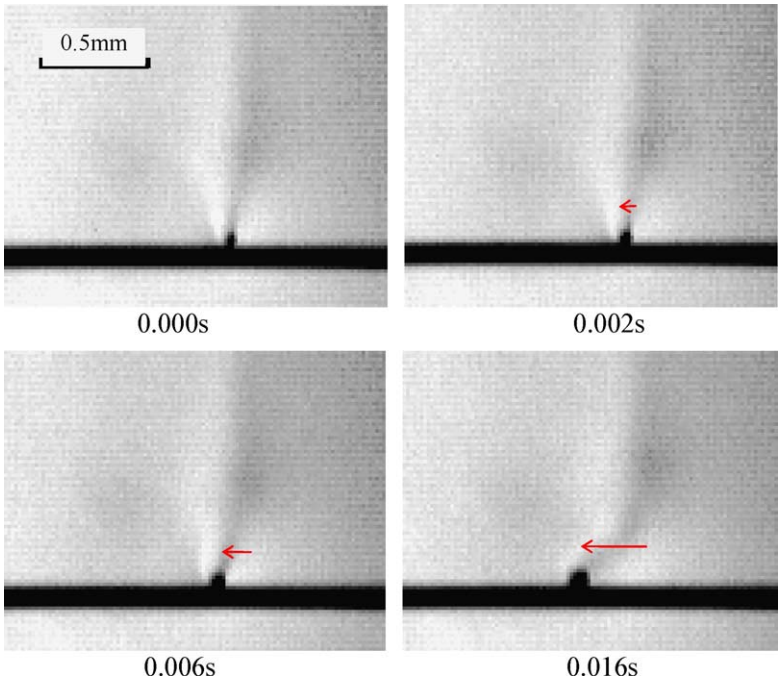

Fig. 7. Bubble slippage startup.

the velocity 20 mm s^{-1} within 0.16, and then moved at the constant velocity of 20 mm s^{-1}. During this period, the acceleration of the bubble decreased from about 2.5 m s^{-2} to 0.

3. Thermocapillary force

Wang et al. [13,14] qualitatively discussed the possible reasons of bubble sweeping phenomenon, and considered the thermocapillary effect as a dominant driving force. Actually, this effect was noted in different investigations [15,16], though it was not considered as an important factor in many cases due to the existence of buoyancy. Takahashi et al. [17] found that thermocapillary effect around a bubble was very strong and played an important role in driving liquid flow around a bubble and other microscale processes. Marangoni or thermocapillary effect always causes liquid convection from higher to lower temperature region along the interface and generates the attraction force on the bubble toward the higher temperature region. This may be expected to result in various bubble motions on a heating wire and to be discussed as an emphasized aspect in this investigation.

Forces applying on a bubble should include the thermocapillary force induced by the bulk liquid temperature difference, inertial force and drag force due to viscous and bubble movement. Most of the theoretical studies of thermocapillary migration in available literature [18,19] were devoted to investigating the quasi-stationary motion. However, for bubble collision and/or oscillation phenomenon, the inertia and non-stationary motion also play important roles in bubble dynamics.

Consider a bubble submerged in an unbounded viscous Newtonian fluid having 1-D temperature profile, as shown in Fig. 9. The temperature difference between two sides of a bubble in the liquid could induce thermocapillary effect. Apparently, the reverse force of the momentum transfer due to the Marangoni flow would push the bubble to move toward high temperature region, and the drive force in x-direction is expressed as

$$f_d = -\int_0^{\pi} \frac{\partial \sigma(T_i)}{\partial T_i} \frac{dT_i}{R\,d\theta} 2\pi R \sin\theta \sin\theta R\,d\theta \tag{1}$$

The temperature gradient along the bubble interface would be

$$\frac{dT_i}{R\,d\theta} = \frac{dT_i}{dx}\frac{dx}{R\,d\theta} = \frac{dT_i}{dx}\sin\theta \tag{2}$$

The relation between the interface temperature gradient $dT_i(x)/dx$ and the bulk temperature gradient $dT(x)/dx$ should be determined by the interfacial condition of $\lambda_l dT/dr|_{r=R} = h_i(T_i - T_{sat}) = q''$ [20] and local heat transfer. As an initial approach for theoretical investigation, the temperature gradient along the interface of small bubbles has linear relation with the bulk temperature gradient as

$$dT_i(x)/dx = \alpha\, dT(x)/dx \quad 0 < \alpha < 1 \tag{3}$$

where α is a dimensionless coefficient.

The function of the interfacial tension as temperature is [20]

$$\sigma(T_i) = \sigma(T_0) - B(T_i - T_0) \tag{4}$$

where $\sigma(T_0)$ is the interfacial tension at temperature T_0, B a positive constant.

For small bubble on thin wire, the external temperature can be normally assumed linear as $T = T_0 + Dx + f(y)$, where T_0 is a reference temperature, and D, D' temperature gradient in x- and y-direction, respectively. Substituting Eqs. (2) and (3) into Eq. (1) and integrating yields

$$f_d = \frac{8}{3}\pi\alpha DBR^2 \tag{5}$$

The temperature gradient D in the liquid can be caused by the external heating and cold source or the bubble motion itself. During subcooled boiling on a thin wire, there are many bubbles standing or moving on the wire, and they can all be important external sources for each other. Fig. 10a illustrates a photo of immobile bubbles and jet flow phenomena during subcooled boiling on a thin wire, where the liquid temperature was 30 °C and heat flux was 1.20×10^6 W m^{-2}. In most experiments, the flow structure nearby bubbles can be described as Fig. 10b, and there is also a temperature gradient along horizontal direction. The neighbor bubbles normally act as cold sources due to evaporation existing at the interface. In another view, since

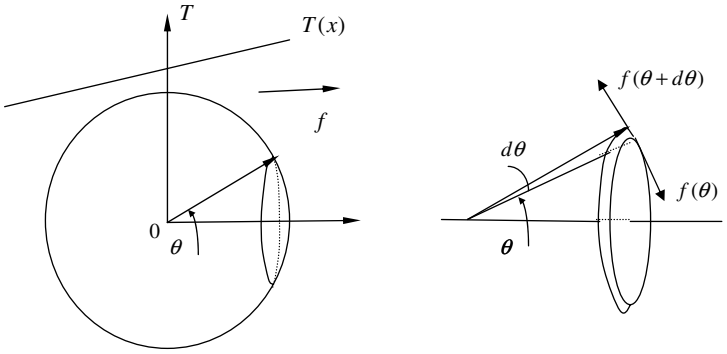

Fig. 9. Thermal drive force on a bubble.

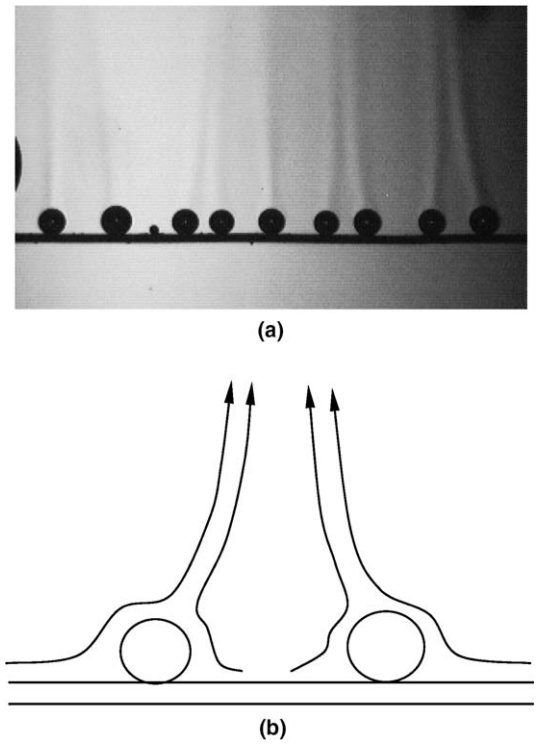

Fig. 10. Interaction among bubbles: (a) immobile bubbles and their interaction and (b) streamline of jet flows of two neighbor bubbles.

the liquid flow around a bubble tends to the neighbor bubbles, it should have an impact that drives the bubble away from the neighbor bubble.

4. Bubble dynamics

4.1. Force caused by bubble motion

To investigate the thermocapillary force induced by bubble movement, consider a bubble moving on a wire with cross-section area A and perimeter C, as illustrated in Fig. 11. The energy equation of the wire could be

$$\rho cA\frac{\partial T}{\partial \tau}=\frac{\partial}{\partial x}\left[\lambda_w A\frac{\partial T}{\partial x}\right]+q_3'-h(T_w-T_b)C \tag{6a}$$

where q_3' is wire heat generation, T_w, T_b the temperatures of the wire surface and bulk liquid, respectively. Assume that the bubble just acts as a heat sink, q_4, at the section x_b, and the heat balance is

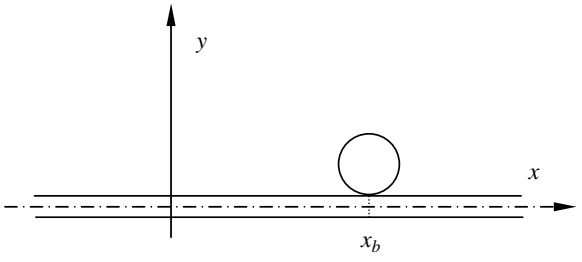

Fig. 11. Temperature with a moving bubble sink.

$$-\lambda_w A\left.\frac{\partial T}{\partial x}\right|_{x=x_b^-}+\lambda_w A\left.\frac{\partial T}{\partial x}\right|_{x=x_b^+}=q_4 \tag{6b}$$

Eq. (6) can be rewritten as [22],

$$\frac{\partial \theta}{\partial \tau}=\kappa\left(\frac{\partial^2\theta}{\partial x^2}-b^2\theta\right)+\frac{q_3'''}{\rho c} \tag{7a}$$

$$-\left.\frac{\partial \theta}{\partial x}\right|_{x=x_b^-}+\left.\frac{\partial \theta}{\partial x}\right|_{x=x_b^+}=\frac{q_4}{\lambda_w A} \tag{7b}$$

where $\theta=T_w-T_b$, $b=\sqrt{hC/\lambda_w A}$, $q_3'''=q_3'/A$, and κ is the thermal diffusion coefficient. As a preliminary approach, b is assumed as a constant.

Set moving coordinates at the bubble, and substituting $x'=x-u\tau$, $\tau'=\tau$ into Eq. (7) yields

$$\frac{\partial \theta}{\partial \tau'}-u\frac{\partial \theta}{\partial x'}=\kappa\left(\frac{\partial^2\theta}{\partial x'^2}-b^2\theta\right)+\frac{q_3'''}{\rho c} \tag{8a}$$

$$-\left.\frac{\partial \theta}{\partial x}\right|_{x'=0^-}+\left.\frac{\partial \theta}{\partial x}\right|_{x'=0^+}=\frac{q_4}{\lambda_w A} \tag{8b}$$

Considering the bubble moving as a steady process, or $\partial\theta/\partial\tau'=0$, we have [21]

$$-u\frac{\partial \theta}{\partial x'}=\kappa\left(\frac{\partial^2\theta}{\partial x'^2}-b^2\theta\right)+\frac{q_3'''}{\rho c} \tag{9}$$

Solving Eq. (9) yields [22]

$$\begin{aligned}&\theta=\phi_{\max}\exp\left\{\left[\sqrt{\left(\frac{u}{2\kappa}\right)^2+b^2}-\frac{u}{2\kappa}\right]x'\right\}+\frac{q_3'''A}{hC},\quad \text{as } x'<0\\&\theta=\phi_{\max}\exp\left\{\left[-\sqrt{\left(\frac{u}{2\kappa}\right)^2+b^2}-\frac{u}{2\kappa}\right]x'\right\}+\frac{q_3'''A}{hC},\quad \text{as } x'>0\end{aligned} \tag{10}$$

where $\phi_{\max}=\frac{-q_4}{2\lambda_w A\sqrt{\left(\frac{u}{2\kappa}\right)^2+b^2}}$. From Eq. (10), the liquid temperature in the front region of the sliding bubble is higher than that behind the bubble, so the thermocapillary force induced by bubble motion itself would act as a drive force, which is opposite to the liquid viscous force.

In the small bubble zone, the temperature gradient for $x'<0$ and $x'>0$ caused by bubble motion is assumed to be uniform and taken as $\partial\theta/\partial x'|_{x'\to 0^-}$ and $\partial\theta/\partial x'|_{x'\to 0^+}$, respectively. From Eqs. (5) and (10), thermocapillary forces for these two zones are

$$\begin{aligned}f_{db1}&=\frac{4}{3}\pi\alpha BR^2\left.\frac{\partial\theta}{\partial x'}\right|_{x'\to 0^+}\\&=\frac{4}{3}\pi\alpha BR^2\phi_{\max}\left[-\sqrt{\left(\frac{u}{2\kappa}\right)^2+b^2}-\frac{u}{2\kappa}\right],\quad x'>0\end{aligned} \tag{11a}$$

$$\begin{aligned}f_{db2}&=\frac{4}{3}\pi\alpha BR^2\left.\frac{\partial\theta}{\partial x'}\right|_{x'\to 0^-}\\&=\frac{4}{3}\pi\alpha BR^2\phi_{\max}\left[\sqrt{\left(\frac{u}{2\kappa}\right)^2+b^2}-\frac{u}{2\kappa}\right],\quad x'<0\end{aligned} \tag{11b}$$

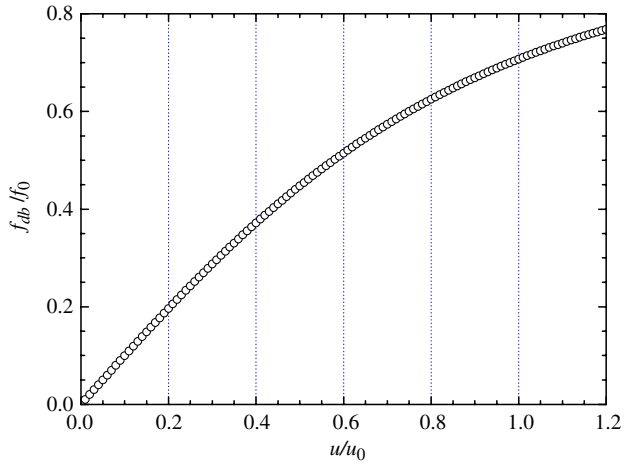

Fig. 12. Thermocapillary force induced by bubble motion.

where f_{db1} and f_{db2} means the thermocapillary force before and behind the bubble, respectively.

As a result, the total thermocapillary force caused by the bubble motion is

$$f_{db} = f_{db1} + f_{db2} = -\frac{4}{3}\pi\alpha B R^2 \phi_{max}\frac{u}{\alpha} \tag{12}$$

or

$$f_{db} = \frac{4}{3}\pi\alpha B R^2 \frac{-q_4}{2\lambda_w A\sqrt{\left(\frac{u}{2\kappa}\right)^2 + b^2}}\frac{u}{\kappa} \tag{13}$$

Fig. 12 presents the variation of the thermocapillary force with bubble velocity, where $u_0 = 2\kappa b$, and $f_0 = -\frac{4}{3}\frac{\pi\alpha B R^2 q_4}{\lambda_w A}$. Corresponding to the experimental conditions, we have $\kappa = 2.503\times10^{-5}\ \mathrm{m^2/s}$, $\lambda_w = 71.4\ \mathrm{W\,m^{-2}}$, $A/C = r/2 = 2.5\times10^{-5}\ \mathrm{m}$, $h = (0.1\text{–}1)\times10^5\ \mathrm{W\,m^{-2}\,K^{-2}}$ (here $h = 0.5\times10^5\ \mathrm{W\,m^{-2}}$), and then $u_0 = 263\ \mathrm{mm\,s^{-1}}$. In most experiments, the velocity of a moving bubble is usually less than $100\ \mathrm{mm\,s^{-1}}$ or $u/u_0 < 0.38$. So the thermocapillary force caused by bubble motion would have a good linear relation with the velocity, or can be expressed as

$$f_{db} \approx \frac{2}{3}\frac{\pi\alpha B R^2 q_4}{\lambda_w A\kappa b}u \tag{14}$$

For pure vapor bubbles in these experiments, the viscous force is given by the Hadamard–Rybczynski law [23], or

$$f_{vl} = -4\pi\mu_l R u \tag{15}$$

where μ_l is the liquid viscosity. Finally, the viscous and thermocapillary effect caused by bubble motion is

$$f_v = \left(-4\pi\mu_l R + \frac{2}{3}\frac{\pi\alpha B R^2 q_4}{\lambda_w A\kappa b}\right)u \tag{16}$$

If the effect caused by bubble motion is considered as effectual viscosity and similar to Stokes' law, it can be expressed as

$$f_v = -6\pi\mu R u \tag{17}$$

where $\mu = \frac{2}{3}\mu_l - \frac{\alpha B R q_4}{9\lambda_w A\kappa b}$ is the effectual viscosity.

4.2. Bubble dynamic equation

When a bubble accelerates or decelerates, the inertial effect is very important in the bubble motion. For a sphere submerged in water, the equivalent inertial mass of the liquid is [24]

$$m_a = \frac{1}{2}\rho_l V \tag{18}$$

and then the total inertial mass is

$$m = m_a + \rho_g V \tag{19}$$

For $\rho_l \gg \rho_g$, the inertia mass in the liquid is

$$m = \frac{1}{2}\rho_l\frac{4}{3}\pi R^3 = \frac{2}{3}\pi\rho_l R^3 \tag{20}$$

In addition, the inertial force is derived as

$$ma = \frac{2}{3}\pi\rho_l R^3 a \tag{21}$$

From Eqs. (5), (16) and (21), the dynamical equation of a moving bubble on a heating wire is derived as

$$ma = \frac{2}{3}\pi\rho_l R^3 a = -6\pi\mu R u + \frac{8}{3}\pi\alpha D B R^2 \tag{22a}$$

or

$$a = -ku + c \tag{22b}$$

where $k = \frac{9\mu}{\rho_l R^2}$ is relative effectual viscosity, $c = \frac{4\alpha B D}{\rho_l R}$ acceleration caused by the external thermocapillary force. Apparently, the bubble dynamic process is controlled by the effectual viscosity force and external thermocapillary force.

4.3. Bubble slippage behavior

For stable bubble slippage without external temperature gradient effect along horizontal direction, $D = 0$, $c = 0$, and then

$$a = -ku \tag{23}$$

From Eq. (23) we have,

$$u = u_0\exp(-kt) \tag{24}$$

Obviously, the effectual viscosity μ or k governs the bubble slippage. The slippage distance will be

$$l = \frac{u_0}{k}[1 - \exp(-kt)] = \frac{u_0}{k}\left[1 - \frac{u}{u_0}\right] \tag{25}$$

Consider a bubble slippage process similar to Fig. 5, $u_0 \approx 64\ \mathrm{mm\,s^{-1}}$, $l \approx 2.8\ \mathrm{mm}$, $\rho_l \approx 1000\ \mathrm{kg\,m^{-3}}$, $R = 0.31$ mm, and for a small velocity variation like $u/u_0 = 0.98$, then $\mu \approx 4.6\times10^{-6}\ \mathrm{kg\,s^{-1}m^{-1}}$. As a result, the effectual viscosity is much less than the viscosity in bubble motions.

From Eq. (22), the whole dynamic characteristics were mainly determined by the effectual viscosity and external conditions, such as D. The effectual viscosity can be rewritten from Eq. (17) as

$$\mu = \frac{2}{3}\mu_l - \frac{\alpha B}{9\pi\sqrt{2\lambda_w h}\kappa}\frac{q_4}{R^{1/2}} \tag{26}$$

Obviously, the effectual viscosity is dependent of the heat sink intensity and bubble radius. Let $\mu = 0$ in Eq. (26), we have

$$\frac{q_4}{R^{1/2}} = \frac{6\pi\sqrt{2\lambda_w h}\kappa}{\alpha B}\mu_l = k_0 \tag{27}$$

For $q_4 R^{-1/2} > k_0$ or $\mu < 0$, a little perturbation will magnify according to Eq. (24), and the immobile bubble under this condition will be unstable and begin to start. For bubble slippage startup process in Fig. 7, the bubble significantly grew up due to quickly absorbing heat, $q_4 R^{-1/2} > k_0$ or $\mu < 0$, and apparently the bubble would accelerate. This process experienced two stages as in shown Fig. 8. In first 0.003 s, the initial velocity was very small, however, the acceleration increased very fast. After that, the acceleration decreased and the velocity approached to a constant value. At about 0.016 s, the acceleration approximated to zero, and the bubble reached its stable slippage process, as described by Eq. (27).

For $q_4 R^{-1/2} < k_0$ or $\mu > 0$, the bubble velocity would tend to zero quickly according to Eq. (23), and the boiling system would almost only have immobile bubbles, which can be usually observed at low heat fluxes, as illustrated in Fig. 2a. For $q_4 R^{-1/2} > k_0$ or $\mu < 0$, from Eq. (22) it is known that the bubble would quickly accelerate and violent collision would cause the bubbles unstable and departing fast. As applied heat flux increases, the bubbles could not keep on the wire because of very high bubble density and acceleration, which corresponds to the small bubble jet phenomenon in Fig. 2b.

Only for $q_4 R^{-1/2} \approx k_0$ or $\mu \approx 0$, the bubble velocity would not magnify or reduce significantly, and the bubble behavior is mainly governed by various external conditions. In this case, the bubble moves along the wire stably and freely with small effectual viscosity, and complex and interesting bubble phenomena occur, as illustrated in Fig. 3.

5. Conclusions

Both experimental observation and theoretical analysis were conducted to understand bubble slippage phenomenon, and the dynamical models are proposed to describe the bubble dynamics, particularly bubble slippage for the subcooled liquid boiling on very small heating wires. The bubble was observed sliding on the thin wire for a long distance with almost constant velocity. According to the experimental results, interfacial thermocapillary force played an important role in the bubble dynamics. The force caused by bubble motion could be handled as the effectual viscosity including liquid viscosity and thermocapillary force. The bubble dynamic equation was derived considering the effectual viscous effect and external thermocapillary force. The behavior of the stable bubble slippage and its startup process were theoretically investigated using bubble dynamical models, and different bubble dynamical phenomena were also described and discussed. The theoretical results are in a reasonable agreement with the experimental observations.

Acknowledgements

This research is currently supported by Specialized Research Fund for the Doctoral Program of Higher Education (Contract No. 20040003076).

References

[1] J.G. Leidenfrost, De Aquea communis nonnullis qualitatibus tractatus, Duisburg, 1756 (C. Wares, Trans.), Int. J. Heat Mass Transfer 9 (1966) 1153.
[2] S. Nukiyama, Maximum and minimum value of heat transmitted from a metal to boiling water under atmosphere pressure, Int. J. Heat Mass Transfer 27 (1984) 959–970.
[3] H.K. Forster, N. Zuber, Dynamics of vapor bubble and boiling heat transfer, AIChE J. 1 (1952) 531–535.
[4] K.H. Sun, J.H. Lienhard, The peak pool boiling heat flux on horizontal cylinders, Int. J. Heat Mass Transfer 13 (1970) 1425–1439.
[5] R. Cole, S.J.D. Van Stralen, Boiling Phenomena, Hemisphere Publishing Corp., Washington, DC, 1979.
[6] G.E. Thorncroft, J.F. Klausner, R. Mei, An experimental investigation of bubble growth and detachment in vertical upflow and downflow boiling, Int. J. Heat Mass Transfer 41 (1998) 3857–3871.
[7] Y.A. Buyevich, B.W. Webbon, Dynamics of vapour bubbles in nucleate boiling, Int. J. Heat Mass Transfer 39 (1996) 2409–2426.
[8] J. Straub, Microscale boiling heat transfer under 0 g and 1 g conditions, Int. J. Thermal Sci. 39 (2000) 490–497.
[9] P.G. Deng, Y.K. Lee, P. Cheng, The growth and collapse of a microbubble under pulse heating, Int. J. Heat Mass Transfer 46 (2003) 4041–4050.
[10] J.Y. Jung, J.Y. Lee, H.C. Park, H.Y. Kwak, Bubble nucleation on micro line heaters under steady or finite pulse of voltage input, Int. J. Heat Mass Transfer 46 (2003) 3897–3907.
[11] A. Asai, T. Hara, I. Endo, One-dimensional models of bubble growth and liquid flow in bubble jet printer, Jpn. J. Appl. Phys. 26 (1987) 1794–1801.
[12] K. Cornwell, I.A. Grant, Heat transfer to bubbles under horizontal tubes, Int. J. Heat Mass Transfer 41 (1998) 1189–1197.
[13] H. Wang, X.F. Peng, B.X. Wang, D.J. Lee, Bubble sweeping and jet flows during nucleate boiling of subcooled liquids, Int. J. Heat Mass Transfer 46 (2003) 863–869.
[14] H. Wang, X.F. Peng, B.X. Wang, D.J. Lee, Bubble-sweeping mechanisms, Sci. Sina, Ser. E 46 (2003) 225–233.
[15] L. Lin, Selective encapsulations of MEMS: micro channels, needles, resonators and electromechanical filters, Ph.D. thesis, University of California, Berkeley, 1999.
[16] T.K. Jun, C.J. Kim, Valveless pumping using traversing vapor bubbles in microchannels, J. Appl. Phys. 83 (1998) 5658–5664.
[17] K. Takahashi, J.G. Weng, C.L. Tien, Marangoni effect in microbubble systems, Microscale Themophys. Eng. 3 (1999) 169–182.
[18] N.O. Young, J.S. Goldstein, M.J. Block, The motion of bubbles in a vertical temperature gradient, J. Fluid Mech. 6 (1959) 350–356.
[19] R.S. Subramanian, Transport Processes in Bubbles, Drops and Particles, Hemisphere Pub. Corp., New York, 1992.
[20] V.P. Carey, Liquid–Vapor Phase-Change Phenomena: An Introduction to the Thermophysics of Vaporization and Condensation Processes in Heat Transfer Equipment, Hemisphere Pub. Corp., New York, 1992.

[21] D. Rosenthal, The theory of moving sources of heat and its application to metal treatments, Trans. ASME 68 (1946) 849–866.
[22] E.R.G. Eckert, Heat and Mass Transfer, McGraw-Hill Book Co., Inc., New York, 1959.
[23] J.I. Romas, Lumped models of gas bubbles in thermal gradients, Appl. Math. Model. 21 (1997) 371–386.
[24] T.E. Faber, Fluid Dynamic for Physicists, Cambridge University Press, Cambridge, 2001.